LA-UR-18-29150
Approved for public release; distribution is unlimited.

Title: Design, analysis and preliminary numerical results for the nonconforming VEM for parabolic problems

Author(s): Manzini, Gianmarco
Vacca, Giuseppe

Intended for: Report

Issued: 2018-09-26

Design, analysis and preliminary numerical results for the nonconforming VEM for parabolic problems

G. Manzini [a] and G. Vacca [b]

[a] *Group T-5, Theoretical Division, Los Alamos National Laboratory, Los Alamos, New Mexico, USA;* e-mail: gmanzini@lanl.gov
[b] *Dipartimento di Matematica e Applicazioni, Università di Milano Bicocca, Milano, Italy.*

Abstract

The virtual element method (VEM) is a numerical methodology for solving partial differential equations on unstructured polytopal meshes. In this work, we extend the nonconforming high-order formulation suitable to time-dependent diffusion problems with possibly nonlinear forcing terms. Coupling high-order virtual element formulations in space with time-marching schemes based on Backward Differention Formulas (BDFs) makes a fully discrete method with optimal order of convergence in the Method of Lines framework. We investigate and assess the performance of the method thorugh theoretical analysis and a set of numerical experiments.

Key words: nonconforming virtual element, time-dependent problems, parabolic problems, polyhedral meshes, polygonal mesh

1. Introduction

In the last decade, the scientific literature concerning the numerical approximation of partial differential equations has been characterized by the growing interest in methods that use polygonal and polyhedral meshes instead of triangular and quadrilateral or tetrahedral and hexahedral grids. This interest in the literature is also reflected in commercial and production codes that have recently included polytopal meshes or implement special gridding techniques such as FLOW3D (see [48] for an application to saturated-unsaturated groundwater flow simulations). Indeed, numerical formulations suited to polytopal meshes offer a number of significant advantages such as a simpler meshing of the domain, also including local mesh adaptivity and nonconforming grids without requiring any special treatment for the hanging nodes.

A very effective approach to design numerical methods for polytopal meshes is provided by the virtual element method (VEM), which was proposed in [7] as a variational reformulation of the *nodal* mimetic finite difference (MFD) method [16, 21, 31, 40, 43, 45] for solving diffusion problems on unstructured polygonal meshes. A survey on the MFD method can be found in the review paper [44] and the research monograph [17]. The VEM inherits the flexibility of the MFD method with respect to the admissible meshes, and, inspite of its recent origin, significant new developments have already taken place, see, for example, [3, 4, 8–15, 18–20, 22–25, 27–29, 32, 47, 52, 53]. Moreover, the connection between VEM and finite elements on polygonal/polyhedral meshes is thoroughly investigated in [35, 37, 46], and between VEM and BEM-based FEM method in [34]. The VEM was originally formulated in [7] as a conforming FEM for the Poisson problem. It was later extended to convection-reaction-diffusion problems with variable coefficients in [2, 14]. Meanwhile, the nonconforming formulation for diffusion problems was proposed in [6] as the finite element reformulation of [42] and later extended to general elliptic problems [36], convection-

dominated advection-diffusion-reaction equations [26], Stokes problem [33], eigenvalue problems [38, 39, 51], and the biharmonic equation [5, 54].

In this article, we extend the non-conforming VEM to two-dimensional parabolic problems such as the time-dependent diffusion equation with possibly nonlinear forcing terms. The VEM is based on two discrete bilinear forms, which respectively approximate the "grad-grad" bilinear form of the pure elliptic case and the L^2 scalar product. This latter is built by using the enhancements technique. We investigate the convergence of the time-dependent approximation by deriving an estimate of the approximation error in the semi-discrete and fully discrete case. High-order in time is provided in the Method of Lines framework by coupling the VEM in space with high-order time-marching Backward Differentiation Formulas (BDFs). Numerical tests confirm the theoretical results.

The outline of the paper is as follows. In Section 2, we introduce the continuous problem. In Section 3, we present the nonconforming virtual element method. In Section 4, we investigate the convergence of the method. In Section 5, we assess the performance of the nonconforming VEM through a set of numerical experiments on different families of polygonal meshes. In Section 6, we offer final comments and conclusions.

2. The continuous problem and its virtual element discretization

In this section, we describe the continuous model problem and introduce the semi-discrete virtual element approximation. Throughout the paper, we use the notation of Sobolev spaces, norms and seminorms detailed in [1]. In particular, the symbols $|\cdot|_{s,\omega}$ and $\|\cdot\|_{s,\omega}$ are the seminorm and the norm of the Sobolev space $H^s(\omega)$ defined on the open bounded subset ω of $\mathbb{R}^d$, and $(\cdot,\cdot)_\omega$ is the L^2-inner product. If ω is the whole computational domain Ω, the subscript may be omitted and we may denote the Sobolev seminorm and norm by $|\cdot|_s$ and $\|\cdot\|_s$, and the L^2-inner product by $(\cdot,\cdot)$.

Let $\Omega \subset \mathbb{R}^d$ for $d = 2, 3$ be an open polytopal domain with Lipschitz boundary Γ. Consider the time-dependent diffusion equation with scalar constant coefficient for the unknown variable u: *Find* $u : \Omega \times [0,T] \to \mathbb{R}$ *such that*

$$u_t - \Delta u = f(u,t) \qquad \text{in } \Omega, \text{ for } t \in (0,T], \tag{1}$$

$$u = 0 \qquad \text{on } \Gamma, \text{ for } t \in (0,T], \tag{2}$$

$$u(\cdot,t) = u_0 \qquad \text{in } \Omega, \tag{3}$$

where u_t denotes the time derivative of u, $f(u,t)$ is the forcing term, which we assumed to be Lipschitz continuous in the first argument, and u_0 is the solution at the initial time $t = 0$. To ease the exposition, in the mathematical formulation of the method and its convergence analysis we consider only the case of Dirichlet boundary conditions. Indeed, the extension of our numerical method to other kind of boundary conditions is deemed straightforward. Furthermore, the performance of the method for nonhomogeneous Dirichlet boundary conditions is illustrated in the section of the numerical experiments. The variational formulation of problem (1)-(3) reads as: *Find* $u \in L^2(0,T;H_0^1(\Omega))$ *with* $u_t \in L^2(0,T;H^{-1}(\Omega))$ *such that*

$$m(u_t(t),v) + a(u(t),v) = \langle f(u,t),v\rangle \qquad \forall v \in H_0^1(\Omega), \quad \text{for a. e. } t \in (0,T), \tag{4}$$

$$u(0) = u_0, \tag{5}$$

where the bilinear forms $m, a : V \times V \to \mathbb{R}$ are defined by

$$m(u,v) = \int_\Omega uv \, d\mathbf{x}, \tag{6}$$

$$a(u,v) = \int_\Omega \nabla u \cdot \nabla v \, d\mathbf{x}, \tag{7}$$

and $\langle\cdot,\cdot\rangle$ denotes the duality product between $H^{-1}(\Omega)$ and $H_0^1(\Omega)$ (or, in $L^2(\Omega)$).

The Poincaré inequality and the boundary conditions imply that the H^1 seminorm is actually a norm on $H_0^1(\Omega)$, equivalent to the usual H^1 norm. Therefore, problem (4)-(5) has a unique solution due to the coercivity and continuity of the bilinear form a on $H_0^1(\Omega)$ and the assumption that f is Lipschitz continuous with respect to u [50].

The virtual element semi-discretization of problem (4)-(5) reads as [6]: *Find* $u_h \in L^2(0,T;V_k^h)$ *with* $u_{h,t} \in L^2(0,T;V_k^h)$ *such that*

$$m_h(u_{h,t}(t), v_h) + a_h(u_h(t), v_h) = (f_h(t), v_h) \quad \forall v_h \in V_k^h, \text{ for a.e. } t \in (0,T), \tag{8}$$

$$u_h(0) = u_{h,0}, \tag{9}$$

where V_k^h is the nonconforming virtual element space and m_h, a_h, f_h, $u_{h,0}$ are the approximation in the VEM setting of the L^2-inner product, the bilinear form a, the source term f, and the initial solution $u(0)$, respectively. The next section is devoted to the definition of these mathematical objects and the discussion of their properties.

3. The nonconforming virtual element method

In this section, we first introduce the family of mesh decompositions of the computational domain and the mesh regularity assumptions; then, we define the non-conforming virtual element space (and related approximation properties) that we need for the proper formulation of the virtual element method, cf. [6].

3.1. *Mesh definition and regularity assumptions*

Let $\mathcal{T} = \{\Omega_h\}_h$ be a family of decompositions of Ω into nonoverlapping polytopal elements P with nonintersecting boundary $\partial\mathsf{P}$, center of gravity $\mathbf{x}_\mathsf{P}$, d-dimensional measure $|\mathsf{P}|$, and diameter $h_\mathsf{P} = \sup_{\mathbf{x},\mathbf{y}\in\mathsf{P}} |\mathbf{x}-\mathbf{y}|$. The subindex h that labels each mesh Ω_h is the maximum of the diameters h_P of the elements of that mesh. The boundary of P is formed by straight edges when $d = 2$ and flat faces when $d = 3$. The midpoint and length of each edge e are denoted by $\mathbf{x}_e$ and h_e, respectively. The center of gravity, diameter and area of each face f are denoted by $\mathbf{x}_f$, h_f, and $|f|$, respectively. Sometimes we may refer to the geometric objects forming the elemental boundary $\partial\mathsf{P}$ by the term *side* instead of *edge/face*, and adopt a unified notation by using the symbol σ instead of e or f regardless of the number of spatial dimensions. Accordingly, $\mathbf{x}_\sigma$, h_σ, and $|\sigma|$ denote the center of gravity, diameter, and measure of side σ.

We denote the unit normal vector to the elemental boundary $\partial\mathsf{P}$ by $\mathbf{n}_\mathsf{P}$, and the unit normal vector to edge e, face f and side σ by $\mathbf{n}_e$, $\mathbf{n}_f$, $\mathbf{n}_\sigma$, respectively. Each vector $\mathbf{n}_\mathsf{P}$ points out of P and the orientation of $\mathbf{n}_e$, $\mathbf{n}_f$, and $\mathbf{n}_\sigma$ is fixed *once and for all* in every mesh Ω_h. Finally, $\mathcal{E}_h$, $\mathcal{F}_h$, and $\mathcal{S}_h$ denote the set of edges, faces, and sides of the skeleton of Ω_h. We may distinguish between *internal* and *boundary* sides by using the superscript 0 and ∂. Therefore, $\mathcal{S}_h^0$ is the set of the internal sides, $\mathcal{S}_h^\partial$ the set of the boundary sides, and, obviously, $\mathcal{S}_h^0 \cap \mathcal{S}_h^\partial = \emptyset$ and $\mathcal{S}_h = \mathcal{S}_h^0 \cup \mathcal{S}_h^\partial$.

Now, we state the mesh regularity assumptions that are required for the convergence analysis. Since the method cannot be used simultaneously for $d = 2$ and $d = 3$ and, hence, no ambiguity is possible in such sense, we may refer to the two- and three-dimensional case using the same label **(A0)** and the same symbol γ to denote the *mesh regularity constant*. Note that the assumptions for $d = 2$ can be derived from those for $d = 3$ by reducing the spatial dimension.

(A0) Mesh regularity assumptions.

- $\mathbf{d = 3}$. A positive constant ϱ independent of h (and, hence, of Ω_h) exists such that for every polyhedral element $\mathsf{P} \in \Omega_h$ it holds that
  (i) P is star-shaped with respect to a ball of internal points of P with radius $\geq \varrho h_\mathsf{P}$;
  (ii) every face $f \in \mathsf{P}$ is star-shaped with respect to a disk of internal points of f with radius $\geq \varrho h_f$;
  (iii) for every edge $e \in \partial f$ of every face $f \in \partial\mathsf{P}$ it holds that $h_e \geq \varrho h_f \geq \varrho^2 h_\mathsf{P}$.
- $\mathbf{d = 2}$. A positive constant ϱ independent of h (and, hence, of Ω_h) exists such that for every polygonal element $\mathsf{P} \in \Omega_h$ it holds that
  (i) P is star-shaped with respect to a disk of internal points of P with radius $\geq \varrho h_\mathsf{P}$;
  (ii) for every edge $e \in \partial\mathsf{P}$ it holds that $h_e \geq \varrho h_\mathsf{P}$.

Remark 3.1 *The star-shapedness property implies that elements and faces are* simply connected *subsets of $\mathbb{R}^d$ and $\mathbb{R}^{d-1}$, respectively. The scaling assumption implies that the number of edges and faces in each elemental boundary is uniformly bounded over the whole mesh family $\mathcal{T}$.*

3.2. *Basic setting*

We introduce the broken Sobolev space for any $s > 0$

$$H^s(\Omega_h) = \prod_{\mathsf{P}\in\Omega_h} H^s(\mathsf{P}) = \big\{\, v \in L^2(\Omega) \,:\, v_{|\mathsf{P}} \in H^s(\mathsf{P}) \,\big\},$$

and define the broken H^s-norm

$$\|v\|_{s,h}^2 = \sum_{\mathsf{P}\in\Omega_h} \|v\|_{s,\mathsf{P}}^2 \qquad \forall\, v \in H^s(\Omega_h), \tag{10}$$

and for $s = 1$ the broken H^1-seminorm

$$|v|_{1,h}^2 = \sum_{\mathsf{P}\in\Omega_h} \|\nabla v\|_{0,\mathsf{P}}^2 \qquad \forall\, v \in H^1(\Omega_h). \tag{11}$$

Let $\sigma \subset \partial\mathsf{P}_\sigma^+ \cap \partial\mathsf{P}_\sigma^-$ be the internal side (edge/face) shared by elements P_σ^+ and P_σ^-, and v a function that belongs to $H^1(\Omega)$. We denote the traces of v on σ from the interior of elements $\mathsf{P}_\sigma^\pm$ by $v_\sigma^\pm$, and the unit normal vectors to σ pointing from $\mathsf{P}_\sigma^\pm$ to $\mathsf{P}_\sigma^\mp$ by $\mathbf{n}_\sigma^\pm$. Then, we introduce the jump operator $[\![\, v \,]\!] = v_\sigma^+\mathbf{n}_\sigma^+ + v_\sigma^-\mathbf{n}_\sigma^-$ at each internal side $\sigma \in \mathcal{S}_h^0$, and $[\![\, v \,]\!] = v_\sigma\mathbf{n}_\sigma$ at each boundary side $\sigma \in \mathcal{S}_h^\partial$. The nonconforming space $H^{1,nc}(\Omega_h;k)$ for any integer $k \geq 1$ is the subspace of the broken Sobolev space $H^1(\Omega_h)$ defined as

$$H^{1,nc}(\Omega_h;k) = \left\{ v \in H^1(\Omega_h) \,:\, \int_\sigma [\![\, v \,]\!] \cdot \mathbf{n}_\sigma\, q\, d\sigma = 0 \;\; \forall\, q \in \mathbb{P}_{k-1}(\sigma),\; \forall\sigma \in \mathcal{S}_h \right\}. \tag{12}$$

Since $[\![\, v \,]\!] = 0$ on any mesh side and $v_\Gamma = 0$ (in the sense of the trace theorem) whenever v belongs to $H_0^1(\Omega)$, it trivially follows that $H_0^1(\Omega) \subset H^{1,nc}(\Omega_h;k)$.

Hereafter, we consider the extension of the bilinear form $a(\cdot,\cdot)$ to the broken Sobolev space $H^1(\Omega_h)$, which is given by splitting it as sum of local terms:

$$a : H^1(\Omega_h) \times H^1(\Omega_h) \to \mathbb{R} \;\text{ such that}$$

$$a(u,v) = \sum_{\mathsf{P}\in\Omega_h} a^{\mathsf{P}}(u,v) \;\text{ where }\; a^{\mathsf{P}}(u,v) = \int_{\mathsf{P}} \nabla u \cdot \nabla v \, d\mathbf{x}, \quad \forall u, v \in H^1(\Omega_h). \tag{13}$$

Clearly, the same definition applies when at least one entry of $a(\cdot,\cdot)$ belongs to the nonconforming space $H^{1,nc}(\Omega_h;k)$, which is a subspace of $H^1(\Omega_h)$, and the nonconforming virtual element space, which will be defined in the next section as a subspace of $H^{1,nc}(\Omega_h;k)$.

The nonconforming space with $k = 1$ has the minimal regularity required for the VEM formulation and the convergence analysis. It is straightforward to show that $|\cdot|_{1,h}$ is a norm on $H^{1,nc}(\Omega_h;k)$, although it is only a seminorm for the discontinuous functions of $H^1(\Omega_h)$. Moreover, using the Poincaré-Friedrichs inequality $\|v\|_0^2 \leq C_{PF}|v|_{1,h}^2$, which holds for every $v \in H^{1,nc}(\Omega_h;k)$ and some positive constant C_{PF} independent of h, cf. [30], we can show that $|\cdot|_{1,h}$ is equivalent to $\|\cdot\|_{1,h}$. Therefore, we may refer to the seminorm $|\cdot|_{1,h}$ as a norm in $H^{1,nc}(\Omega_h;k)$.

According to [6], if $u \in H^s(\Omega)$ with $s \geq 3/2$ and for any $v \in H^{1,nc}(\Omega_h;k)$ we find that

$$\mathcal{N}_h(u(t),v) = m(u_t(t),v) + a(u,v) - \langle f, v\rangle = \sum_{\sigma\in\mathcal{S}_h} \int_\sigma \nabla u \cdot [\![\, v \,]\!]\, ds. \tag{14}$$

The quantity $\mathcal{N}_h(u,v)$ is called the *conformity error*.

We now recall an estimate for the term measuring the nonconformity.

Lemma 3.2 (See [6]) *Assume **(A0)** is satisfied. Let $u \in H^{1+s}(\Omega)$ with $1 \leq s \leq k$ be the solution of* (4)-(5)*. Let $v \in H^{1,nc}(\Omega_h;k)$, $k \geq 1$, as defined in* (12)*. Then, there exists a positive constant $\mathcal{C}$ independent of h such that*

$$|\mathcal{N}_h(u,v)| \leq Ch^s|u|_{1+s}|v|_{1,h}, \tag{15}$$

where $\mathcal{N}_h(u,v)$ is defined in (14)*. Constant $\mathcal{C}$ depends on the polynomial degree k and the mesh regularity factor γ.*

Throughout the paper, $\mathbb{P}_\ell(D)$ denotes the space of polynomials of degree up to ℓ for any integer number $\ell \geq 0$ on the bounded connected subset D of $\mathbb{R}^\nu$ with $\nu = 1, 2, 3$. The polynomial space $\mathbb{P}_\ell(D)$ is finite dimensional and we denote its dimension by $\pi_{\ell,\nu}$. It holds that $\pi_{\ell,1} = \ell + 1$ for $\nu = 1$; $\pi_{\ell,2} = (\ell+1)(\ell+2)/2$ for $\nu = 2$; $\pi_{\ell,3} = (\ell+1)(\ell+2)(\ell+3)/6$ for $\nu = 3$. We also conventionally take $\mathbb{P}_{-1}(D) = \{0\}$ and $\pi_{-1,\nu} = 0$ for every integer $\nu > 0$. Let $\mathbf{x}_D$ denote the center of gravity of D and h_D its characteristic length, as, for instance, the edge length for $\nu = 1$, the face diameter for $\nu = 2$ and the cell diameter for $\nu = 3$. A basis for $\mathbb{P}_\ell(D)$ is provided by $\mathcal{M}_\ell(D) = \{ (\mathbf{x} - \mathbf{x}_D)/h_D)^\alpha \text{ with } |\alpha| \leq \ell \}$, the set of the *scaled monomials of degree up to* ℓ, where $\alpha = (\alpha_1, \ldots \alpha_\nu)$ is a ν-dimensional multi-index of nonnegative integers α_i with degree $|\alpha| = \alpha_1 + \ldots + \alpha_\nu$ and such that $\mathbf{x}^\alpha = x_1^{\alpha_1} \ldots x_\nu^{\alpha_\nu}$ for any $\mathbf{x} \in \mathbb{R}^\nu$. We will also use the set of *scaled monomials of degree exactly equal to* ℓ, denoted by $\mathcal{M}_\ell^*(D)$ and obtained by setting $|\alpha| = \ell$ in the definition of $\mathcal{M}_\ell(D)$. Finally, we denote by $\Pi_\ell^0 : L^2(\mathsf{P}) \to \mathbb{P}_\ell(\mathsf{P})$ for $\ell \geq 0$ the L^2-orthogonal projection onto the polynomial space $\mathbb{P}_\ell(\mathsf{P})$, and by $\Pi_\ell^{0,\sigma} : L^2(\sigma) \to \mathbb{P}_\ell(\sigma)$ for $\ell \geq 0$ the L^2-orthogonal projection onto the polynomial space $\mathbb{P}_\ell(\sigma)$.

3.3. *Local and global nonconforming virtual element space*

We construct the local nonconforming virtual element space by resorting to the so-called *enhancement strategy* originally devised in [2] for the conforming VEM and later extended to the nonconforming VEM in [36]. To this end, for any polytopal cell $\mathsf{P} \in \Omega_h$ and integer number $k \geq 1$, we first define the finite dimensional functional space

$$\widetilde{V}_k^h(\mathsf{P}) = \left\{ v \in H^1(\mathsf{P}) \,:\, \frac{\partial v}{\partial \mathbf{n}} \in \mathbb{P}_{k-1}(\sigma)\, \forall \sigma \subset \partial\mathsf{P},\, \Delta v \in \mathbb{P}_k(\mathsf{P}) \right\}. \tag{16}$$

The space $\widetilde{V}_k^h(\mathsf{P})$ contains the polynomials of degree k.

Then, we introduce the set of continuous linear functionals from $\widetilde{V}_k^h(\mathsf{P})$ to $\mathbb{R}$ that for every virtual function v_h of $\widetilde{V}_k^h(\mathsf{P})$ provide:

(D1) the moments of v_h of order up to $k-1$ on each $(d-1)$-dimensional side $\sigma \in \partial\mathsf{P}$:

$$\frac{1}{|\sigma|} \int_\sigma v_h\, m\, ds,\ \forall m \in \mathcal{M}_{k-1}(\sigma),\, \forall \sigma \in \partial\mathsf{P}; \tag{17}$$

(D2) the moments of v_h of order up to $k-2$ on P:

$$\frac{1}{|\mathsf{P}|} \int_\mathsf{P} v_h\, m\, d\mathbf{x}, \quad \forall m \in \mathcal{M}_{k-2}(\mathsf{P}). \tag{18}$$

Finally, we introduce the elliptic projection operator $\Pi_k^\nabla : \widetilde{V}_k^h(\mathsf{P}) \to \mathbb{P}_k(\mathsf{P})$ that for any $v_h \in \widetilde{V}_k^h(\mathsf{P})$ is defined by:

$$\int_\mathsf{P} \nabla \Pi_k^\nabla v_h \cdot \nabla q\, d\mathbf{x} = \int_\mathsf{P} \nabla v_h \cdot \nabla q\, d\mathbf{x} \qquad \forall q \in \mathbb{P}_k(\mathsf{P}) \tag{19}$$

together with the additional conditions:

$$\int_{\partial\mathsf{P}} (\Pi_k^\nabla v_h - v_h)\, ds = 0 \qquad \text{if } k = 1, \tag{20}$$

$$\int_\mathsf{P} (\Pi_k^\nabla v_h - v_h)\, d\mathbf{x} = 0 \qquad \text{if } k \geq 2. \tag{21}$$

As proved in [36], the polynomial projection $\Pi_k^\nabla v_h$ is computable using only the values from the linear functionals **(D1)**-**(D2)**. Furthermore, Π_k^∇ is a polynomial-preserving operator, i.e., $\Pi_k^\nabla q = q$ for every $q \in \mathbb{P}_k(\mathsf{P})$.

We are now ready to introduce the *local nonconforming virtual element space of order* k on the polytopal element P, which is the subspace of $\widetilde{V}_k^h(\mathsf{P})$ defined as follow:

$$V_k^h(\mathsf{P}) = \left\{ v \in \widetilde{V}_k^h(\mathsf{P}) \text{ such that } (v_h - \Pi_k^\nabla v_h, m)_\mathsf{P} = 0\ \forall m \in \mathcal{M}_{k-1}^*(\mathsf{P}) \cup \mathcal{M}_k^*(\mathsf{P}) \right\}. \tag{22}$$

Space $V_k^h(\mathsf{P})$ has the two important properties that we outline below:

(i) it still contains the space of polynomials of degree at most k;

(ii) the values provided by the set of continuous linear functionals **(D1)-(D2)** uniquely determine every function v_h of $V_k^h(\mathsf{P})$ and can be taken as the *degrees of freedom* of v_h.

Property (i) above is a direct consequence of the space definition, while property (ii) follows from the unisolvence of the degrees of freedom **(D1)-(D2)** that was proved in [6, 36]. Additionally, the L^2-orthogonal projection $\Pi_k^0 v_h$ is computable using the degrees of freedom of v_h, cf. [36], and $\Pi_k^0 v_h = \Pi_k^\nabla v_h$ for $k = 1, 2$ as for the conforming VEM, cf. [2].

Finally, the *global nonconforming virtual element space* V_k^h *of order* $k \geq 1$ *subordinate to the mesh* Ω_h is obtained by gluing together the elemental spaces $V_k^h(\mathsf{P})$ to form a subspace of the nonconforming space $H^{1,nc}(\Omega_h; k)$. The formal definition reads as:

$$V_k^h := \Big\{ v_h \in H^{1,nc}(\Omega_h; k) \ : \ v_{h|\mathsf{P}} \in V_k^h(\mathsf{P}) \ \ \forall \mathsf{P} \in \Omega_h \Big\}. \tag{23}$$

A set of degrees of freedom for V_k^h is given by collecting the values from the linear functionals **(D1)** for all the mesh sides and **(D2)** for all the mesh elements. The unisolvence of degrees of freedom (17)-(18) for V_k^h is an immediate consequence of their unisolvence on each local space $V_k^h(\mathsf{P})$. Thus, the dimension of V_k^h is equal to $N^{\mathcal{S}} \times \pi_{k-1,d-1} + N^{\mathcal{P}} \times \pi_{k-2,d}$, where $N^{\mathcal{S}}$ is the total number of sides, and $\pi_{\ell,\nu}$ is the dimension of the space of polynomials of degree up to ℓ in $\mathbb{R}^\nu$.

Remark 3.3 *The set of degrees of freedom can be properly redefined by excluding the moments on the* $N^{\mathcal{S},\partial}$ *boundary sides, i.e., for* $\sigma \in \mathcal{S}_h^\partial$*, which are set to zero to impose the homogeneous Dirichlet boundary condition* (2)*. This reduces the dimension of* V_k^h *to* $N^{\mathcal{S},0} \times \pi_{k-1,d-1} + N^{\mathcal{P}} \times \pi_{k-2,d}$*.*

3.4. *Approximation properties*

Both for completeness of exposition and future reference in the paper, we briefly summarize a few local approximation properties for the virtual nonconforming space. We omit here any detail about the derivation of these estimates and refer the interested readers to References [2, 6, 7] and the references therein.

Local polynomial approximations. On a given element $\mathsf{P} \in \Omega_h$, consider the function $v \in H^s(\mathsf{P})$ with $1 \leq s \leq k+1$. Under mesh assumptions **(A0)**, there exists a piecewise polynomial approximation that is of degree k on each element, i.e., v_π, such that

$$\|v - v_\pi\|_{0,\mathsf{P}} + h_\mathsf{P} |v - v_\pi|_{1,\mathsf{P}} \leq C h_\mathsf{P}^s |v|_{s,\mathsf{P}}, \tag{24}$$

for some constant $C > 0$ that may only depend on the polynomial degree k and the mesh regularity constant ϱ.

An instance of such a local polynomial approximation is provided by the L^2-projection $\Pi_k^0 v$ onto the local polynomial space $\mathbb{P}_k(\mathsf{P})$, which necessarily satisfies the (optimal) error bound:

$$\|v - \Pi_k^0 v\|_{0,\mathsf{P}} + h_\mathsf{P} |v - \Pi_k^0 v|_{1,\mathsf{P}} \leq C h_\mathsf{P}^s |v|_{s,\mathsf{P}}, \tag{25}$$

for some constant $C > 0$ that may only depend on the polynomial degree k and the mesh regularity constant ϱ.

Furthermore, consider the internal side $\sigma \in \mathcal{S}_h^0$ and let $\mathsf{P}^\pm$ be the two elements sharing σ, so that $\sigma = \partial\mathsf{P}^+ \cap \partial\mathsf{P}^-$. We denote $\Omega_\sigma = \mathsf{P}^+ \cup \mathsf{P}^-$. Then, for every $w \in H^s(\Omega_\sigma)$ with $1 \leq s \leq k+1$, the L^2-projection $\Pi_k^{0,\sigma} v$ onto $\mathbb{P}_k(\sigma)$, the space of polynomials of degree k on side σ, satisfies the error estimate

$$\|v - \Pi_k^{0,\sigma} v\|_{0,\sigma} + h_\sigma |v - \Pi_k^{0,\sigma} v|_{1,\sigma} \leq C h_\sigma^{s-\frac{1}{2}} |v|_{s,\Omega_\sigma}. \tag{26}$$

The same estimate holds also for the boundary sides $\sigma \in \mathcal{S}_h^\partial$ by taking $\Omega_\sigma = \mathsf{P}$, the element to which σ belongs.

Interpolation error. Similarly, under mesh regularity assumptions **(A0)**, we can define an interpolation operator in V_k^h having optimal approximation properties. Therefore, for every $v \in H^s(\mathsf{P})$ with $1 \leq s \leq k+1$ we can find the local interpolate $v^\mathrm{I} \in V_k^h(\mathsf{P})$, which is the virtual element function that has the same degrees of freedom of v on the mesh element P. The interpolate v^I is an approximation of v and the approximation error in the L^2 and H^1 norms is estimated as

$$\|v - v^\mathrm{I}\|_{0,\mathsf{P}} + h_\mathsf{P} |v - v^\mathrm{I}|_{1,\mathsf{P}} \leq C h_\mathsf{P}^s |v|_{s,\mathsf{P}}, \tag{27}$$

where $C > 0$ is a positive constant independent of h.

3.5. *Virtual element semi-discretization*

The discrete bilinear forms $a_h(\cdot,\cdot)$ and $m_h(\cdot,\cdot)$ are given by the sum of elemental contributions

$$m_h(u_h, v_h) = \sum_{\mathsf{P}\in\Omega_h} m_h^P(u_h, v_h), \tag{28}$$

$$a_h(u_h, v_h) = \sum_{\mathsf{P}\in\Omega_h} a_h^P(u_h, v_h), \tag{29}$$

where

$$m_h^P(u_h, v_h) = m^{\mathsf{P}}(\Pi_k^0 u_h, \Pi_k^0 v_h) + S_m^{\mathsf{P}}\Big((I-\Pi_k^0)u_h, (I-\Pi_k^0)v_h\Big), \tag{30}$$

and

$$a_h^P(u_h, v_h) = a^{\mathsf{P}}(\Pi_k^\nabla u_h, \Pi_k^\nabla v_h) + S_a^{\mathsf{P}}\Big((I-\Pi_k^\nabla)u_h, (I-\Pi_k^\nabla)v_h\Big), \tag{31}$$

and $S_m^{\mathsf{P}}(\cdot,\cdot)$ and $S_a^{\mathsf{P}}(\cdot,\cdot)$ can be any two symmetric and positive definite bilinear forms such that

$$\widehat{\mu}_* (v_h, v_h)_{\mathsf{P}} \le S_m^{\mathsf{P}}(v_h, v_h) \le \widehat{\mu}^* (v_h, v_h)_{\mathsf{P}} \quad \forall v_h \in V_k^h(\mathsf{P}) \text{ with } \Pi_k^0 v_h = 0, \tag{32}$$

for some pair of positive constants $\widehat{\mu}_*$ and $\widehat{\mu}^*$, and

$$\widehat{\alpha}_* a^{\mathsf{P}}(v_h, v_h) \le S_a^{\mathsf{P}}(v_h, v_h) \le \widehat{\alpha}^* a^{\mathsf{P}}(v_h, v_h) \quad \forall v_h \in V_k^h(\mathsf{P}) \text{ with } \Pi_k^\nabla v_h = 0, \tag{33}$$

for some pair of positive constant $\widehat{\alpha}_*$ and $\widehat{\alpha}^*$. From the conditions above it follows immediately that $S_m^{\mathsf{P}}(\cdot,\cdot)$ scales like $(\cdot,\cdot)_{\mathsf{P}}$, i.e., $S_m^{\mathsf{P}}(\cdot,\cdot) \simeq h_{\mathsf{P}}^d$, and, similarly, that $S_a^{\mathsf{P}}(\cdot,\cdot)$ scales like $a^{\mathsf{P}}(\cdot,\cdot)$, i.e., $S_a^{\mathsf{P}}(\cdot,\cdot) \simeq h_{\mathsf{P}}^{d-2}$.

The discrete bilinear forms $m_h(\cdot,\cdot)$ and $a_h(\cdot,\cdot)$ need to satisfy the following properties:

- *k-consistency*: for all $v_h \in V_k^h$ and for all $q \in \mathbb{P}_k(\mathsf{P})$ it holds

$$m_h^P(v_h, q) = (v_h, q)_{\mathsf{P}}\,, \tag{34}$$

$$a_h^P(v_h, q) = a^{\mathsf{P}}(v_h, q); \tag{35}$$

- *stability*: there exists two pairs of positive constants (μ_*, μ^*) and $(\alpha_*,\ \alpha^*)$, independent of h and P, such that

$$\mu_* (v_h, v_h)_{\mathsf{P}} \le m_h^P(v_h, v_h) \le \mu^* (v_h, v_h)_{\mathsf{P}} \quad \forall v_h \in V_k^h, \tag{36}$$

$$\alpha_* a^{\mathsf{P}}(v_h, v_h) \le a_h^P(v_h, v_h) \le \alpha^* a^{\mathsf{P}}(v_h, v_h) \quad \forall v_h \in V_k^h. \tag{37}$$

In particular, the first term in the definition of m_h^P in (30) and a_h^P in (31) provides the k-consistency, and, hence, determines the accuracy of the method; the second one ensures its stability (see also [6]). For both bilinear forms, the k-consistency property follows immediately from definitions (30) and (31) since the stabilization terms are zero whenever one of their entries is a polynomial. Stability easily follows from a straightforward calculation by taking $\mu^* = \max(1, \widehat{\mu}^*)$, $\mu_* = \min(1, \widehat{\mu}_*)$, $\alpha^* = \max(1, \widehat{\alpha}^*)$, and $\alpha_* = \min(1, \widehat{\alpha}_*)$, cf. [7].

We assume that the right-hand side of (4) is given by the sum of local contributions:

$$\langle f_h, v_h\rangle = \sum_{P\in\Omega_h} \left(\Pi_k^0 f, v_h\right)_{\mathsf{P}}\,, \tag{38}$$

where on each element P we approximate f by its L^2-orthogonal projection $\Pi_k^0 f$ on the polynomials of degree up to k. We use the same local projection to approximate the nonlinear dependence of f on the solution u in its first argument; hence,

$$f(u,t) \approx f_h(u_h, t) := \Pi_k^0 f(\Pi_k^0 u_h, t).$$

	α_1	α_0	α_{-1}	α_{-2}	α_{-3}	β
BDF_1	1	-1				1
BDF_2	1	$-\frac{4}{3}$	$\frac{1}{3}$			$\frac{2}{3}$
BDF_3	1	$-\frac{18}{11}$	$\frac{9}{11}$	$-\frac{2}{11}$		$\frac{6}{11}$
BDF_4	1	$-\frac{48}{25}$	$\frac{36}{25}$	$-\frac{16}{25}$	$\frac{3}{25}$	$\frac{12}{25}$

Table 1. *Coefficients of the BDF^s method used in the full discrete approximation* (41).

Each local term is fully computable for any nonlinear integrable function $f(u,t)$ and any function v_h in V_k^h since the orthogonality property implies that

$$\big(\Pi_k^0 f(\Pi_k^0 u_h, t), v_h\big)_{\mathsf{P}} = \big(\Pi_k^0 f(\Pi_k^0 u_h, t), \Pi_k^0 v_h\big)_{\mathsf{P}} = \big(f(\Pi_k^0 u_h, t), \Pi_k^0 v_h\big)_{\mathsf{P}},$$

and both $\Pi_k^0 u_h$ and $\Pi_k^0 v_h$ are computable from their degrees of freedom. Using the L^2-orthogonal projection in the numerical treatment of the right-hand side does not change its regularity. Indeed, for any two functions $v_h, w_h \in V_k^h$ the continuity of the orthogonal projection Π_k^0 implies that

$$\begin{aligned} \|f_h(v_h,t) - f_h(w_h,t)\|_{\mathsf{P}} &= \|\Pi_k^0 f(\Pi_k^0 v_h, t) - \Pi_k^0 f(\Pi_k^0 w_h, t)\|_{\mathsf{P}} = \big\|\Pi_k^0\big(f(\Pi_k^0 v_h, t) - f(\Pi_k^0 w_h, t)\big)\big\|_{\mathsf{P}} \\ &\leq \|f(\Pi_k^0 v_h, t) - f(\Pi_k^0 w_h, t)\|_{\mathsf{P}}, \end{aligned} \tag{39}$$

and the Lipschitz continuity of f_h follows from the Lipschitz continuity of f.

Let N^{dofs} denote the number of degrees of freedom of the VEM. For the symmetry and stability conditions of the bilinear forms a_h and m_h and the regularity assumption on f_h, there exist a set of eigenvalues in increasing orders

$$0 < \lambda_h^{(1)} \leq \ldots \leq \lambda^{(N^{\text{dofs}})}$$

and corresponding eigenfunctions $\big\{\omega_h^{(i)}\big\}_{i=1}^{N^{\text{dofs}}}$, which form an orthonormal basis of V_k^h with respect to $m_h(\cdot,\cdot)$, such that

$$a_h(\omega_h^{(i)}, v_h) = \lambda_h^{(i)} m_h(\omega_h^{(i)}, v_h) \qquad v_h \in V_k^h, \quad \text{for } i = 1, \ldots, N^{\text{dofs}}.$$

The unique solvability of the virtual element approximation (8)-(9) is stated by the following theorem.

Theorem 3.4 *Problem* (8)-(9) *has a unique solution given by:*

$$u_h(t) = \sum_{i=1}^{N^{dofs}} \left(m_h(u_{h,0}, \omega_h^{(i)}) e^{-\lambda_h^{(i)} t} + \int_0^t \langle f_h(u_h, \tau), \omega_h^{(i)} \rangle e^{-\lambda_h^{(i)}(t-\tau)}\, d\tau \right) \omega_h^{(i)}.$$

3.6. *Time-stepping scheme*

Here, we briefly describe the time-stepping BDF scheme for our problem. An introduction to these schemes can be found in several textbooks such as [49]. BDF schemes are implicit linear multi-step methods for ordinary differential equations that at any given time approximate the derivative $u_{h,t}(t)$ by using the values of $u_h(t)$ from previous time-steps, thereby increasing the accuracy of the approximation. The semi-discrete approximation leads to a system of ordinary differential equation in the indipendent variable t, which formally reads as

$$\frac{d\underline{u}_h(t)}{dt} = \underline{F}\big(t, \underline{u}_h(t)\big), \tag{40}$$

where vector $\underline{u}_h(t)$ collects all the time dependent degrees of freedom of unknown virtual element approximation $u_h(t)$ and the right-hand side term $\underline{F}\big(t, \underline{u}_h(t)\big)$ collects the constributions from the discrete bilinear form $a_h(u_h(t), \cdot)$ and the right-hand side $(f_h(t), \cdot)$ of equation (8). To discretize this equation with respect to the time variable t, we denote the time-step by Δt^n and the value of the virtual element approximation $u_h(t^n)$ at time $t^n = n\Delta t^k$ for any integer $n \geq 0$ by u_h^n. Then, we approximate the time-derivative of $\underline{u}_h(t)$ and the right-hand side of (40) as follows:

$$u_{h,t}(t^n) \approx \frac{1}{\Delta t^n} \sum_{l=-s+1}^{1} \alpha_l u_h^{n+l} = \beta F(t^{n+1}, u_h^{n+1}), \tag{41}$$

where α_l and β are the coefficients of the *s-stage* BDF, denoted by BDF(s), and are chosen so that the combined BDF(s)-VEM(k) method may achieve optimal accuracy. These coefficients are given in Table 3.6, where we use the notation BDF_s for $s = 1, \ldots, 4$ to denote the number of steps s of the method. Note that BDF_1 corresponds to the backward Euler scheme.

4. Error analysis

We introduce the energy projection $\mathcal{P}^h : H_0^1(\Omega) \to V_k^h$ such that for every $u \in H_0^1(\Omega)$, the virtual element function $\mathcal{P}^h u$ is the solution of the variational problem:

$$a_h(\mathcal{P}^h u, v) = a(u, v_h) \quad \forall v_h \in V_k^h. \tag{42}$$

The energy projection $\mathcal{P}^h u$ is an approximation of u and an estimate of the corresponding approximation error is provided by the following lemma.

Lemma 4.1 *Let $u \in H^{s+1}(\Omega) \cap H_0^1(\Omega)$, with $1 \leq s \leq k$, be the solution of problem* (42) *under the mesh assumptions of Section 3.1. Then, there exists a unique function $\mathcal{P}^h u \in V_k^h$ such that*

$$|u - \mathcal{P}^h u|_{1,h} \leq \mathcal{C} h^s |u|_{s+1}. \tag{43}$$

Moreover, if domain Ω is H^2-regular, it holds that

$$\|u - \mathcal{P}^h u\|_0 \leq \mathcal{C} h^{s+1} |u|_{s+1}. \tag{44}$$

In both equations, the symbol $\mathcal{C}$ denotes a positive constant that is independent of h, but may depend on the mesh regularity factor γ and the stability constants α^*, α_*, μ^*, μ_*.

Proof. The arguments of this proof are similar to those used in the proof of [52, Lemma 3.1], where the conforming VEM is considered for the approximation of the parabolic problem. However, our proof differs in several points due to the nonconforming nature of the space V_k^h considered in this work. In particular, a conformity error appears in the analysis that must be properly estimated.

First, we note that the bilinear form $a_h(\cdot, \cdot)$ is continuous and coercive on $V_k^h \times V_k^h$, the linear functional $a(u, \cdot)$ is continuous on V_k^h, and the Lax-Milgram Lemma implies that the solution $\mathcal{P}^h u$ to problem (42) exists and is unique.

Then, to prove estimate (43), we introduce the virtual element interpolate u^{I} of u, which is the function in V_k^h that has the same degrees of freedom of u and satisfies the error estimate provided by inequality (27). A straightforward application of the triangular inequality yields:

$$|u - \mathcal{P}^h u|_{1,h} \leq |u - u^{\mathrm{I}}|_1 + |u^{\mathrm{I}} - \mathcal{P}^h u|_{1,h}, \tag{45}$$

The first term on the right is estimated by using (27), while to estimate the second term we need the following developments. Let $\delta_h = \mathcal{P}^h u - u^{\mathrm{I}}$ and u_π the piecewise polynomial approximation of degree k that satisfies inequality (24) on each element P. Using the k-consistency property, stability, and the continuity of the bilinear forms a_h and a yield the development chain:

$$\begin{aligned}
\alpha_* |\delta_h|_{1,h}^2 &= \alpha_* a(\delta_h, \delta_h) \leq a_h(\delta_h, \delta_h) = a_h(\mathcal{P}^h u, \delta_h) - a_h(u^{\mathrm{I}}, \delta_h) = a(u, \delta_h) - a_h(u^{\mathrm{I}}, \delta_h) \\
&= \sum_{\mathsf{P} \in \Omega_h} \Big(a^{\mathsf{P}}(u, \delta_h) - a_h^P(u^{\mathrm{I}}, \delta_h) \Big) \\
&= \sum_{\mathsf{P} \in \Omega_h} \Big(a^{\mathsf{P}}(u - u_\pi, \delta_h) - a_h^P(u^{\mathrm{I}} - u_\pi, \delta_h) \Big) \\
&\leq \sum_{\mathsf{P} \in \Omega_h} \Big(|u - u_\pi|_{1,\mathsf{P}} + \alpha^* |u^{\mathrm{I}} - u_\pi|_{1,\mathsf{P}} \Big) |\delta_h|_{1,\mathsf{P}} \\
&\leq \max(1, \alpha^*) \Big(|u - u_\pi|_{1,h} + |u^{\mathrm{I}} - u_\pi|_{1,h} \Big) |\delta_h|_{1,h}.
\end{aligned}$$

Therefore, it holds that

$$|\mathcal{P}^h u - u^{\mathrm{I}}|_{1,h} \leq \frac{\alpha^*}{\alpha_*} \Big(|u - u_\pi|_{1,h} + |u^{\mathrm{I}} - u_\pi|_{1,h} \Big),$$

and substituting this relation in (45) and applying estimates (27) and (24) to the resulting inequality provides estimate (43).

To derive the estimate in the L^2-norm when Ω is an H^2-regular domain we consider the weak solution $\psi \in H_0^1(\Omega)$ to the auxiliary elliptic equation:

$$-\Delta\psi = u - \mathcal{P}^h u \quad \text{in } \Omega, \tag{46}$$

which satisfies the H^2 regularity result:

$$\|\psi\|_2 \leq \mathcal{C}\|u - \mathcal{P}^h u\|_1. \tag{47}$$

Let $\psi^{\mathrm{I}} \in V_k^h$ be the virtual element interpolate of ψ that satisfies estimate (27). We integrate by parts; we note that $[\![u]\!] = 0$ since we have assumed that u is at least in $H^2(\Omega)$; we use the definition of the energy projection $\mathcal{P}^h$; we introduce the conformity error that depends on the jumps of $\mathcal{P}^h u$ at the elements' sides to find that

$$\begin{aligned}
\|u - \mathcal{P}^h u\|_0^2 &= \big(u - \mathcal{P}^h u, u - \mathcal{P}^h u\big) = \big(u - \mathcal{P}^h u, -\Delta\psi\big) \\
&= a(u - \mathcal{P}^h u, \psi) - \sum_{\sigma\in\mathcal{S}_h} \int_\sigma \nabla\psi \cdot [\![u - \mathcal{P}^h u]\!]\, ds \\
&= a(u - \mathcal{P}^h u, \psi - \psi^{\mathrm{I}}) + a(u - \mathcal{P}^h u, \psi^{\mathrm{I}}) + \sum_{\sigma\in\mathcal{S}_h} \int_\sigma \nabla\psi \cdot [\![u - \mathcal{P}^h u]\!]\, ds \\
&= \mathsf{T}_1 + \mathsf{T}_2 + \mathsf{T}_3.
\end{aligned} \tag{48}$$

The proof continues by estimating each term T_i, $i = 1, 2, 3$, separately.

The first term is bounded as follows:

$$\begin{aligned}
|\mathsf{T}_1| = |a(u - \mathcal{P}^h u, \psi - \psi^{\mathrm{I}})| &\leq \|u - \mathcal{P}^h u\|_{1,h}\, \|\psi - \psi^{\mathrm{I}}\|_{1,h} \\
&\leq \mathcal{C}h^s |u|_{s+1}\, h|\psi|_2 \leq \mathcal{C}h^{s+1}|u|_{s+1}\|u - \mathcal{P}^h u\|_0
\end{aligned}$$

where we used the estimate in the energy norm (43) derived previously and the estimate of the interpolation error (27).

For the second term, first we use the consistency and stability property to transform T_2 as follows:

$$\begin{aligned}
\mathsf{T}_2 = a(u, \psi^{\mathrm{I}}) - a(\mathcal{P}^h u, \psi^{\mathrm{I}}) &= \sum_{\mathsf{P}\in\Omega_h} \Big(a_h^P(\mathcal{P}^h u, \psi^{\mathrm{I}}) - a^{\mathsf{P}}(\mathcal{P}^h u, \psi^{\mathrm{I}}) \Big) \\
&= \sum_{\mathsf{P}\in\Omega_h} \Big(a_h^P(\mathcal{P}^h u - u_\pi, \psi^{\mathrm{I}} - \Pi_1^0\psi) - a^{\mathsf{P}}(\mathcal{P}^h u - u_\pi, \psi^{\mathrm{I}} - \Pi_1^0\psi) \Big).
\end{aligned}$$

Then, we add and subtract u and ψ and use estimates (24) and (27) to obtain

$$\begin{aligned}
|\mathsf{T}_2| &\leq \max(1, \alpha^*) \sum_{\mathsf{P}\in\Omega_h} |\mathcal{P}^h u - u_\pi|_{1,\mathsf{P}} |\psi^{\mathrm{I}} - \Pi_1^0\psi|_{1,\mathsf{P}} \\
&\leq \max(1, \alpha^*) \sum_{\mathsf{P}\in\Omega_h} \big(|\mathcal{P}^h u - u|_{1,\mathsf{P}} + |u - u_\pi|_{1,\mathsf{P}} \big) \big(|\psi^{\mathrm{I}} - \psi|_{1,\mathsf{P}} + |\psi - \Pi_1^0\psi|_{1,\mathsf{P}} \big) \\
&\leq \mathcal{C} \sum_{\mathsf{P}\in\Omega_h} h_{\mathsf{P}}^s |u|_{s+1,\mathsf{P}}\, h|\psi|_{2,\mathsf{P}} \leq \mathcal{C}h^{s+1}|u|_{s+1}\|\psi\|_2 \\
&\leq \mathcal{C}h^{s+1}|u|_{s+1}\|u - \mathcal{P}^h u\|_0,
\end{aligned}$$

and the bound of T_2 is derived by using in the final step the H^2-regularity of ψ.

To bound the conformity error we first rewrite the integrals of the jumps as follows:

$$\mathsf{T}_3 = \sum_{\sigma\in\mathcal{S}_h} \int_\sigma \nabla\psi \cdot [\![\mathcal{P}^h u]\!]\, ds = \sum_{\sigma\in\mathcal{S}_h} \int_\sigma \big(I - \Pi_0^{0,\sigma}\big)\nabla\psi \cdot \big(I - \Pi_0^{0,\sigma}\big)[\![u - \mathcal{P}^h u]\!]\, ds.$$

Then, we use the Cauchy-Schwarz inequality, we apply the error estimate of the orthogonal projection of the traces on each side $\sigma \in \mathcal{S}_h$, and we use the estimate in the energy norm (43) previously derived:

$$
\begin{aligned}
|\mathsf{T}_3| &\leq \sum_{\sigma\in\mathcal{S}_h} \|(I-\Pi_1^{0,\sigma})\nabla\psi\cdot\mathbf{n}_\sigma\|_{0,\sigma}\|\big(I-\Pi_0^{0,\sigma}\big)[\![\, u-\mathcal{P}^h u\,]\!]\cdot\mathbf{n}_\sigma\|_{0,\sigma}\\
&\leq \mathcal{C}\sum_{\sigma\in\mathcal{S}_h} h_\sigma^{\frac{1}{2}}|\nabla\psi|_{1,\Omega_\sigma} h_\sigma^{\frac{1}{2}}|u-\mathcal{P}^h u|_{1,\Omega_\sigma} \leq \mathcal{C}h^{s+1}\|\psi\|_2|u|_{s+1} \leq \mathcal{C}h^{s+1}|u|_{s+1}\|u-\mathcal{P}^h u\|_0.
\end{aligned}
$$

Note that we did not used the result of Lemma 3.2, since had we done that we would have lost the extra convergence factors h^s from the estimate in the energy norm of $u-\mathcal{P}^h u$.

The estimate in the L^2-norm is finally proved by collecting the estimates of the three terms T_i, $i=1,2,3$, derived above.

□

Theorem 4.2 *Let $u\in H^{s+1}(\Omega)$, with $1\leq s\leq k$, be the solution of problem* (4)-(5) *and $u_h\in V_k^h$ be the virtual element approximation to u solving* (8)-(9) *under the mesh assumptions of Section* (3.1)*. Then, if the domain Ω is H^2-regular, there exists a positive constant $\mathcal{C}$ independent of h such that*

$$
\|u(t)-u_h(t)\|_0 \leq \|u_0-u_{h,0}\|_0 + \mathcal{C}h^{s+1}\Big(|u_0|_0 + \|u_t\|_{L^2(0,t;H^{s+1}(\Omega))} + \|u\|_{L^2(0,t;H^{s+1}(\Omega))} \tag{49}
$$

$$
+ \|f\|_{L^2(0,t;H^{s+1}(\Omega))}\Big) + \mathcal{C}h^s\|u\|_{L^2(0,t;H^{s+1}(\Omega))} \tag{50}
$$

for almost every t in $(0,T]$. The constant $\mathcal{C}$ may depend on the final time T, the mesh regularity constant γ and the stability constants α_*, α^*, μ_*, μ^*.

Proof. Consider $\theta_h(t)=u_h(t)-\mathcal{P}^h u(t)$, $\rho_h(t)=\mathcal{P}^h u(t)-u(t)$, and the decomposition:

$$
u_h(t)-u(t) = \big[u_h(t)-\mathcal{P}^h u(t)\big] + \big[\mathcal{P}^h u(t)-u(t)\big] = \theta_h(t)+\rho_h(t). \tag{51}
$$

Lemma 4.1 allows us to estimate the projection error $\rho_h(t)$ for a.e. $t\in(0,T]$:

$$
\begin{aligned}
\|\rho_h(t)\|_0 &\leq \mathcal{C}h^{s+1}|u(t)|_{s+1}\\
&\leq \mathcal{C}h^{s+1}\Big|u(0)+\int_0^t u_t(\tau)\,d\tau\Big|_{s+1}\\
&\leq \mathcal{C}h^{s+1}\left(|u_0|_{s+1}+\int_0^t |u_t(\tau)|_{s+1}\,d\tau\right)\\
&\leq \mathcal{C}h^{s+1}\left(|u_0|_{s+1}+\sqrt{T}\left(\int_0^t |u_t(\tau)|_{s+1}^2\,d\tau\right)^{\frac{1}{2}}\right)\\
&= \mathcal{C}h^{s+1}\left(|u_0|_{s+1}+|u_t|_{L^2(0,t;H^{s+1}(\Omega))}\right),
\end{aligned} \tag{52}
$$

where the final constant $\mathcal{C}$ absorbs the factor $\sqrt{T}$.

To bound term $\theta_h(t)$, we start with the error equation:

$$
\begin{aligned}
m_h(\theta_{h,t}(t),v_h)+a_h(\theta_h(t),v_h) &= (f_h(u_h,t),v_h) - m_h(d\mathcal{P}^h u(t)/\,dt,v_h) - a_h(\mathcal{P}^h u(t),v_h)\\
&= (f_h(u_h,t),v_h) - m_h(\mathcal{P}^h u_t(t),v_h) - a(u(t),v_h)\\
&= (f_h(u_h,t),v_h) - m_h(\mathcal{P}^h u_t(t),v_h) + m(u_t(t),v_h) - (f(u,t),v_h) - \mathcal{N}_h(u(t),v_h)\\
&= \Big[(f_h(u_h,t)-f(u,t),v_h)\Big] + \Big[m(u_t(t),v_h)-m_h(\mathcal{P}^h u_t(t),v_h)\Big] + \Big[-\mathcal{N}_h(u(t),v_h)\Big]\\
&= \mathsf{T}_1+\mathsf{T}_2+\mathsf{T}_3.
\end{aligned}
$$

The proof continues by bounding the three terms separately. To ease the notation, we introduce the symbols $\overline{u}=\Pi_k^0 u$ and $\overline{u}_h=\Pi_k^0 u_h$. The continuity of the projection operator Π_k^0 implies that $\|\overline{u}-\overline{u}_h\|_0=\|\Pi_k^0(u-u_h)\|_0\leq\|u-u_h\|_0$.

We transform term T_1 as follows by using the definition of f_h and adding and subtracting $\Pi_k^0 f(\overline{u},t)$ and $\Pi_k^0 f(u,t)$ to the inner product arguments:

$$\begin{aligned}\mathsf{T}_1 &= \sum_{\mathsf{P}\in\Omega_h} (f_h(u_h,t) - f(u,t), v_h)_{\mathsf{P}} = \sum_{\mathsf{P}\in\Omega_h} (\Pi_k^0 f(\overline{u}_h,t) - f(u,t), v_h)_{\mathsf{P}} \\ &= \sum_{\mathsf{P}\in\Omega_h} \Bigg(\Big[\big(\Pi_k^0 f(\overline{u}_h,t) - \Pi_k^0 f(\overline{u},t), v_h\big)_{\mathsf{P}} \Big] + \Big[\big(\Pi_k^0 f(\overline{u},t) - \Pi_k^0 f(u,t), v_h\big)_{\mathsf{P}} \Big] \\ &\qquad + \Big[\big(\Pi_k^0 f(u,t) - f(u,t), v_h\big)_{\mathsf{P}} \Big] \Bigg) = \mathsf{T}_{1,1} + \mathsf{T}_{1,2} + \mathsf{T}_{1,3}. \end{aligned} \tag{53}$$

Then, we bound each sub-term $\mathsf{T}_{1,i}$ with $i = 1,2,3$ separately. To bound the first sub-term, we use the Cauchy-Schwarz inequality, the continuity of the projection operator twice, the property that f is Lipschitz continuous, and the previous estimate on the projection error:

$$\begin{aligned}|\mathsf{T}_{1,1}| &\le \sum_{\mathsf{P}\in\Omega_h} |(\Pi_k^0 f(\overline{u}_h,t) - \Pi_k^0 f(\overline{u},t), v_h)_{\mathsf{P}}| \le \sum_{\mathsf{P}\in\Omega_h} \|\Pi_k^0(f(\overline{u}_h,t) - f(\overline{u},t))\|_{0,\mathsf{P}} \|v_h\|_{0,\mathsf{P}} \\ &\le \sum_{\mathsf{P}\in\Omega_h} \|f(\overline{u}_h,t) - f(\overline{u},t)\|_{0,\mathsf{P}} \|v_h\|_{0,\mathsf{P}} \le \mathcal{C} \sum_{\mathsf{P}\in\Omega_h} \|\overline{u}_h(t) - \overline{u}(t)\|_{0,\mathsf{P}} \|v_h\|_{0,\mathsf{P}} \\ &\le \mathcal{C} \sum_{\mathsf{P}\in\Omega_h} \|u_h(t) - u(t)\|_{0,\mathsf{P}} \|v_h\|_{0,\mathsf{P}} \le \mathcal{C} \|u_h(t) - u(t)\|_0 \|v_h\|_0. \end{aligned}$$

We use the Cauchy-Schwarz inequality, the boundedness of the projection operator, the property of f of being Lipschitz continuous, and the estimate of the projection error to bound the second sub-term:

$$\begin{aligned}|\mathsf{T}_{1,2}| &\le \sum_{\mathsf{P}\in\Omega_h} \big|\big(\Pi_k^0(f(\overline{u},t) - f(u,t)), v_h\big)_{\mathsf{P}}\big| \le \sum_{\mathsf{P}\in\Omega_h} \|\Pi_k^0(f(\overline{u},t) - f(u,t))\|_{0,\mathsf{P}} \|v_h\|_{0,\mathsf{P}} \\ &\le \sum_{\mathsf{P}\in\Omega_h} \|f(\overline{u},t) - f(u,t)\|_{0,\mathsf{P}} \|v_h\|_{0,\mathsf{P}} \le \sum_{\mathsf{P}\in\Omega_h} \|\overline{u}(t) - u(t)\|_{0,\mathsf{P}} \|v_h\|_{0,\mathsf{P}} \\ &\le \sum_{\mathsf{P}\in\Omega_h} \|(I - \Pi_k^0)u(t)\|_{0,\mathsf{P}} \|v_h\|_{0,\mathsf{P}} \le \mathcal{C} \sum_{\mathsf{P}\in\Omega_h} h_{\mathsf{P}}^{s+1} |u(t)|_{s+1,\mathsf{P}} \|v_h\|_{0,\mathsf{P}} \\ &\le \mathcal{C} h^{s+1} |u(t)|_{s+1} \|v_h\|_0 \end{aligned}$$

We use the Cauchy-Schwarz inequality and the estimate of the projection error to bound the third sub-term:

$$\begin{aligned}|\mathsf{T}_{1,3}| &\le \sum_{\mathsf{P}\in\Omega_h} (\Pi_k^0 f(u,t) - f(u,t), v_h)_{\mathsf{P}} \le \sum_{\mathsf{P}\in\Omega_h} \|(I - \Pi_k^0) f(u,t)\|_{0,\mathsf{P}} \|v_h\|_{0,\mathsf{P}} \\ &\le \mathcal{C} \sum_{\mathsf{P}\in\Omega_h} h_{\mathsf{P}}^{s+1} |f(u,t)|_{s+1,\mathsf{P}} \|v_h\|_{0,\mathsf{P}} \le \mathcal{C} h^{s+1} |f(u,t)|_{s+1} \|v_h\|_0. \end{aligned}$$

Collecting the estimates above yields this bound for T_1:

$$|\mathsf{T}_1| \le \mathcal{C}\Big(\|u_h(t) - u(t)\|_0 + h^{s+1}\big(|u(t)|_{s+1} + \|f(t)\|_{s+1}\big)\Big) \|v_h\|_0. \tag{54}$$

We bound the second term of (53) as follows by using the k-consistency property, the Cauchy-Schwarz inequality

$$
\begin{aligned}
\mathsf{T}_2 &= \sum_{\mathsf{P}\in\Omega_h} \Big(m^{\mathsf{P}}(u_t(t), v_h) - m_h^P(\mathcal{P}^h u_t(t), v_h) \Big) \\
&= \sum_{\mathsf{P}\in\Omega_h} \Big(m^{\mathsf{P}}(u_t(t) - \Pi_k^0 u_t(t), v_h) - m_h^P(\mathcal{P}^h u_t(t) - \Pi_k^0 u_t(t), v_h) \Big) \\
&\leq \mathcal{C} \sum_{\mathsf{P}\in\Omega_h} \Big(\|u_t(t) - \Pi_k^0 u_t(t)\|_{0,\mathsf{P}} + \|(\mathcal{P}^h u_t(t) - \Pi_k^0 u_t(t)\|_{0,\mathsf{P}} \Big) \|v_h\|_{0,\mathsf{P}} \\
&\leq \mathcal{C} \sum_{\mathsf{P}\in\Omega_h} \Big(\|u_t(t) - \Pi_k^0 u_t(t)\|_{0,\mathsf{P}} + \|\mathcal{P}^h u_t(t) - u_t(t)\|_{0,\mathsf{P}} + \|u_t(t) - \Pi_k^0 u_t(t)\|_{0,\mathsf{P}} \Big) \|v_h\|_{0,\mathsf{P}} \\
&\leq \mathcal{C} \sum_{\mathsf{P}\in\Omega_h} h_{\mathsf{P}}^{s+1} |u_t(t)|_{s+1,\mathsf{P}} \|v_h\|_{0,\mathsf{P}} \\
&\leq \mathcal{C} h^{s+1} |u_t(t)|_{s+1} \|v_h\|_0.
\end{aligned} \tag{55}
$$

We bound the third term of (53) by using the result of Lemma 3.2

$$
|\mathsf{T}_3| = |\mathcal{N}_h(u, v_h)| \leq h^s |u|_{s+1} \|v_h\|_0. \tag{56}
$$

Collecting the estimates of the three bounds yield:

$$
\begin{aligned}
m_h(\theta_{h,t}(t), v_h) + a_h(\theta_h(t), v_h) \leq \mathcal{C} \Big(&\|u_h(t) - u(t)\|_0 + h^{s+1} \big(|u(t)|_{s+1} + |u_t(t)|_{s+1} + \|f(t)\|_{s+1} \big) \\
&+ h^s |u(t)|_{s+1} \Big) \|v_h\|_0.
\end{aligned} \tag{57}
$$

Now, from the stability of m_h and a_h it follows that

$$
\mu_* \frac{1}{2} \frac{d}{dt} \|\theta_h(t)\|_0^2 = \mu_* m(\theta_{h,t}(t), \theta_h(t)) \leq m_h(\theta_{h,t}(t), \theta_h(t)) \leq m_h(\theta_{h,t}(t), \theta_h(t)) + a_h(\theta_h(t), \theta_h(t))
$$

and setting $v_h = \theta_h(t)$ in (57) yields:

$$
\mu_* \frac{1}{2} \frac{d}{dt} \|\theta_h(t)\|_0^2 \leq \mathcal{C} \|\theta_h(t)\|_0 \Big(\|u(t) - u_h(t)\|_0 + h^{s+1} \Big(|u_t(t)|_{s+1} + |u(t)|_{s+1} + |f(u,t)|_{s+1} \Big) + h^s |u(t)|_{s+1} \Big).
$$

Then, we substitute $\|u(t) - u_h(t)\|_0 \leq \|\theta_h(t)\|_0 + \|\rho_h(t)\|_0$ and we find that

$$
\begin{aligned}
\mu_* \frac{1}{2} \frac{d}{dt} \|\theta_h(t)\|_0^2 \leq \mathcal{C} \|\theta_h(t)\|_0^2 + \mathcal{C} \|\theta_h(t)\|_0 \Big(&\|\rho_h(t)\|_0 + h^{s+1} \Big(|u_t(t)|_{s+1} + |u(t)|_{s+1} + |f(u,t)|_{s+1} \Big) \\
&+ h^s |u(t)|_{s+1} \Big).
\end{aligned}
$$

Using the Young inequality we find

$$
\begin{aligned}
\mu_* \frac{1}{2} \frac{d}{dt} \|\theta_h(t)\|_0^2 &\leq \mathcal{C} \|\theta_h(t)\|_0^2 + \mathcal{C} \frac{1}{2} \|\theta_h(t)\|_0^2 + \mathcal{C} \frac{1}{2} \Big(\|\rho_h(t)\|_0 + h^{s+1} \Big(|u_t(t)|_{s+1} + |u(t)|_{s+1} + |f(u,t)|_{s+1} \Big) \\
&\qquad + h^s |u(t)|_{s+1} \Big)^2 \\
&\leq \mathcal{C} \|\theta_h(t)\|_0^2 + \mathcal{C} \frac{1}{2} \|\theta_h(t)\|_0^2 + \mathcal{C} \frac{1}{2} \Big(\|\rho_h(t)\|_0^2 + h^{2(s+1)} \Big(|u_t(t)|_{s+1}^2 + |u(t)|_{s+1}^2 + |f(u,t)|_{s+1}^2 \Big) \\
&\qquad + h^{2s} |u(t)|_{s+1}^2 \Big).
\end{aligned}
$$

In view of the bound of $\rho_h(t)$ given by (52) and using the Gronwall's lemma (and taking the square root of both sides) we finally find that

$$
\begin{aligned}
\|\theta_h(t)\|_0 \leq \|\theta_h(0)\|_0 + \mathcal{C} h^{s+1} \Big(&\|u_t\|_{L^2(0,t;H^{s+1}(\Omega))} + \|u\|_{L^2(0,t;H^{s+1}(\Omega))} + \|f(u,t)\|_{L^2(0,t;H^{s+1}(\Omega))} \Big) \\
&+ \mathcal{C} h^s \|u\|_{L^2(0,t;H^{s+1}(\Omega))}.
\end{aligned}
$$

Since

$$\|\theta_h(0)\|_0 \leq \mathcal{C}\Big(\|u_{h,0}-u_0\|_0 + h^{s+1}|u_0|_{s+1}\Big)$$

we have

$$\begin{aligned}\|\theta_h(t)\|_0 \leq \mathcal{C}\Big(&\|u_{h,0}-u_0\|_0 \\ &+ h^{s+1}\big(|u_0|_{s+1} + \|u_t\|_{L^2(0,t;H^{s+1}(\Omega))} + \|u\|_{L^2(0,t;H^{s+1}(\Omega))} + \|f(u,t)\|_{L^2(0,t;H^{s+1}(\Omega))}\big) \\ &+ h^s\|u\|_{L^2(0,t;H^{s+1}(\Omega))}\Big)\end{aligned}$$

The assertion of the theorem follows by combining the estimates for $\rho_h(t)$ and $\theta_h(t)$. □

Theorem 4.3 *Let u be the solution of problem* (4)- (5) *and u_h the virtual element approximation solving* (8)-(9)*. Then, for almost every $t \in (0,T]$ the following estimate holds:*

$$|u(t)-u_h(t)|_{1,h} \leq |u_{h,0}-u_0|_{1,h} + \mathcal{C}h^s\Big(|u_0|_{s+1} + \|u_t\|_{L^2(0,t;H^{s+1}(\Omega))}\Big) \tag{58}$$

$$+ \mathcal{C}h^{s+1}\Big(\|f\|_{L^2(0,t;H^{s+1}(\Omega))} + h\|u_t\|_{L^2(0,t;H^{s+1}(\Omega))}\Big). \tag{59}$$

Proof. Consider again $\theta_h(t) = u_h(t) - \mathcal{P}^h u(t)$, $\rho_h(t) = \mathcal{P}^h u(t) - u(t)$, and the error decomposition:

$$|u_h(t)-u(t)|_{1,h} \leq |\theta_h(t)|_{1,h} + |\rho_h(t)|_{1,h}. \tag{60}$$

Using the result of Lemma 4.1 we find that

$$\begin{aligned}\|\rho_h(t)\|_0 &\leq \mathcal{C}h^s|u(t)|_s \\ &\leq \mathcal{C}h^s\Big|u(0) + \int_0^t u_t(\tau)\,d\tau\Big|_s \\ &\leq \mathcal{C}h^s\left(|u_0|_s + \int_0^t |u_t(\tau)|_s\,d\tau\right) \\ &\leq \mathcal{C}h^s\left(|u_0|_s + \sqrt{T}\left(\int_0^t |u_t(\tau)|_s^2\,d\tau\right)^{\frac{1}{2}}\right) \\ &= \mathcal{C}h^s\left(|u_0|_s + |u_t|_{L^2(0,t;H^s(\Omega))}\right),\end{aligned} \tag{61}$$

where the final constant $\mathcal{C}$ absorbs the factor $\sqrt{T}$. By setting $v_h = \theta_{h,t}(t)$ in (57) it follows that

$$\begin{aligned}m_h(\theta_{h,t}(t),\theta_{h,t}(t)) + a_h(\theta_h(t),\theta_{h,t}(t)) \leq \mathcal{C}\Big(&\|u_h(t)-u(t)\|_0 + h^{s+1}\big(|u(t)|_{s+1} + |u_t(t)|_{s+1} + \|f(u,t)\|_{s+1}\big) \\ &+ h^s|u(t)|_{s+1}\Big)\|\theta_{h,t}(t)\|_0.\end{aligned}$$

From the stability properties of the bilinear forms given in (36) and (37) we see that

$$m_h(\theta_{h,t}(t),\theta_{h,t}(t)) \geq \mu_* m(\theta_{h,t}(t),\theta_{h,t}(t)) = \mu_*\|\theta_{h,t}\|_0^2,$$

$$a_h(\theta_h(t),\theta_{h,t}(t)) = \frac{1}{2}\frac{d}{dt}a_h(\theta_h(t),\theta_h(t)) \geq \frac{\alpha_*}{2}\frac{d}{dt}a(\theta_h(t),\theta_h(t)) = \frac{\alpha_*}{2}\frac{d}{dt}|\theta_h|_{1,h}^2,$$

and using these relations and the Hölder inequality we find that

$$\begin{aligned}\mu_*\|\theta_{h,t}\|_0^2 + \frac{1}{2}\frac{d}{dt}|\theta_h(t)|_{1,h}^2 &\leq \mathcal{C}\Big(\|u_h(t)-u(t)\|_0 + h^{s+1}\big(|u(t)|_{s+1} + |u_t(t)|_{s+1} + \|f(u,t)\|_{s+1}\big) \\ &\qquad + h^s|u(t)|_{s+1}\Big)\|\theta_{h,t}\|_0 \\ &\leq \frac{\mathcal{C}}{\epsilon}\Big(\|u_h(t)-u(t)\|_0 + h^{s+1}\big(|u(t)|_{s+1} + |u_t(t)|_{s+1} + \|f(u,t)\|_{s+1}\big) \\ &\qquad + h^s|u(t)|_{s+1}\Big)^2 + \mathcal{C}\epsilon\|\theta_{h,t}\|_0^2 \\ &\leq \frac{\mathcal{C}}{\epsilon}\Big(\|u_h(t)-u(t)\|_0^2 + h^{2(s+1)}\big(|u(t)|_{s+1}^2 + |u_t(t)|_{s+1}^2 + \|f(u,t)\|_{s+1}^2\big) \\ &\qquad + h^{2s}|u(t)|_{s+1}^2\Big) + \mathcal{C}\epsilon\|\theta_{h,t}\|_0^2.\end{aligned}$$

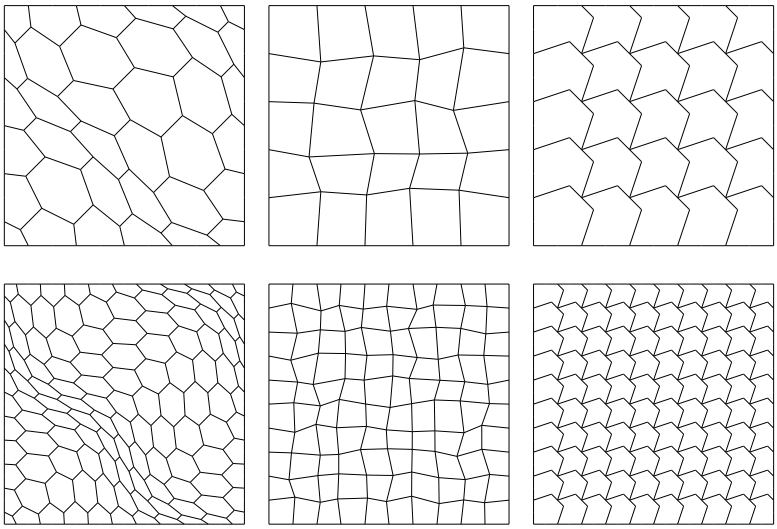

(a) (b) (c)

Fig. 1. Base mesh (top row) and first refinement (bottom row) of the three mesh families: (a) remapped hexagonal mesh; (b) randomly distorted quadrilateral mesh; (c) non-convex regular mesh.

By properly setting ϵ we may remove $\|\theta_{h,t}\|_0^2$ from the inequality above. Then, we integrate in time to obtain:

$$|\theta_h(t)|_{1,h}^2 \leq |\theta_h(0)|_{1,h}^2 + \mathcal{C}\int_0^t \|u_h(s) - u(s)\|_0^2\, ds + \mathcal{C}h^{2(s+1)} \int_0^t \left(|u(t)|_{s+1}^2 + |u_t(t)|_{s+1}^2 + \|f(u,t)\|_{s+1}^2\right) ds + \mathcal{C}h^{2s} \int_0^t |u(t)|_{s+1}^2\, ds.$$

The assertion of the theorem follows by using the estimate for $\|u_h(t) - u(t)\|_0$ provided by Theorem 4.2 and $|\theta_h(0)|_{1,h} = |u_h(0) - \mathcal{P}^h u(0)|_{1,h} = |u_{h,0} - \mathcal{P}^h u_0|_{1,h}$ provided by Lemma 4.1 (cf. (43)), and finally taking the square root of both sides.

□

5. Numerical Results

The numerical experiments of this section are aimed at confirming the convergence rates predicted by the *a priori* analysis developed in the previous sections. In a preliminary stage, the consistency of the numerical method, i.e. the exactness of these methods for polynomial solutions, has been tested numerically by solving the elliptic equation with boundary and source data determined by the monomials $u(x, y) = x^\mu y^\nu$ on different set of polygonal meshes and for all possible combinations of nonnegative integers μ and ν such that $\mu + \nu \leq 3$. In all the cases, the magnitude of the errors was of the order of the arithmetic precision, thus confirming the consistency of the VEM.

To study the accuracy of the method we solve the time-dependent heat equation on the domain $\Omega =]0, 1[\times]0, 1[$. The forcing term and the Dirichlet boundary conditions are set in accordance with the exact solution

$$u(x, y) = \left(\sin(2\pi x)\sin(2\pi y) + x^5 + y^5\right)\cos(2\pi t/T) \tag{62}$$

The performance of the VEM developed in this paper is investigated by evaluating the rate of convergence on three different sequences of unstructured meshes, labeled by $\mathcal{M}_1$, $\mathcal{M}_2$, and $\mathcal{M}_3$, respectively. The top panels of Fig. 1 show the first mesh of each sequence and the bottom panels show the mesh of the first refinement.

The meshes in $\mathcal{M}_1$ are the dual mesh of the mesh obtained by remapping the position $(\widehat{x}, \widehat{y})$ of the nodes of a uniform square partition of Ω by the smooth coordinate transformation [41]:

$$x = \widehat{x} + (1/10)\sin(2\pi\widehat{x})\sin(2\pi\widehat{y}),$$
$$y = \widehat{y} + (1/10)\sin(2\pi\widehat{x})\sin(2\pi\widehat{y}).$$

The meshes in $\mathcal{M}_2$ are obtained by randomly displacing the nodes of a regular mesh of squares. The meshes in $\mathcal{M}_3$ are obtained by filling the computational domain with a suitably scaled non-convex octagonal reference cell. The meshes are parametrised by the number of partitions in each direction. The starting mesh of every sequence is built from a 5×5 regular grid, and the refined meshes are obtained by doubling this resolution. Time integration is provided by coupling the VEM of order k with the marching scheme using the BDF of order $k + 1$ in the method of lines framework.

All errors are reported in Figs. 2, 3, and 4, and are labeled by a circle for $k = 1$, squares for $k = 2$, and diamonds for $k = 3$. Each figure shows the relative errors in the L^2 norms (left panels) and the H^1 norms (right panels). Moreover, the error curves are plotted with respect to the maximum diameter of the discretization in the top panels and with respect to the total number of degrees of freedom in the bottom panels. The expected slopes of the convergence curves are shown directly on the plots. The numerical results confirm the theoretical rate of convergence.

6. Conclusions

The virtual element method (VEM) is a numerical methodology for solving partial differential equations on unstructured polytopal meshes. A nonconforming high-order formulation suitable to time-dependent diffusion problems with possibly nonlinear forcing terms is designed and investigated theoretically and numerically. This formulation combines the high-order VEM in space with high-order time-marching schemes based on backward differention formulas in the method of lines framework. Optimal convergence rates are derived through the theoretical analysis and confirmed by a set of numerical experiments.

Acknowledgements

The work of the first author was partially supported by the Laboratory Directed Research and Development Program (LDRD), U.S. Department of Energy Office of Science, Office of Fusion Energy Sciences, and the DOE Office of Science Advanced Scientific Computing Research (ASCR) Program in Applied Mathematics Research, under the auspices of the National Nuclear Security Administration of the U.S. Department of Energy by Los Alamos National Laboratory, operated by Los Alamos National Security LLC under contract DE-AC52-06NA25396.

References

[1] R. A. Adams. *Sobolev spaces*, volume 65 of *Pure and Applied Mathematics,*. Academic Press, New York-London, 1975.

[2] B. Ahmad, A. Alsaedi, F. Brezzi, L. D. Marini, and A. Russo. Equivalent projectors for virtual element methods. *Computers & Mathematics with Applications*, 66:376–391, September 2013.

[3] P. F. Antonietti, L. Beirão da Veiga, D. Mora, and M. Verani. A stream virtual element formulation of the stokes problem on polygonal meshes. *SIAM Journal on Numerical Analysis*, 52(1):386–404, 2014.

[4] P. F. Antonietti, L. Beirão da Veiga, S. Scacchi, and M. Verani. A C^1 virtual element method for the Cahn-Hilliard equation with polygonal meshes. *SIAM Journal on Numerical Analysis*, 54(1):34–56, 2016.

[5] P. F. Antonietti, G. Manzini, and M. Verani. The fully nonconforming Virtual Element method for biharmonic problems. *Mathematical Models & Methods in Applied Sciences*, 28(2), 2018.

[6] B. Ayuso de Dios, K. Lipnikov, and G. Manzini. The nonconforming virtual element method. *ESAIM: Mathematical Modelling and Numerical Analysis*, 50(3):879–904, 2016.

[7] L. Beirão da Veiga, F. Brezzi, A. Cangiani, G. Manzini, L. D. Marini, and A. Russo. Basic principles of virtual element methods. *Mathematical Models & Methods in Applied Sciences*, 23:119–214, 2013.

[8] L. Beirão da Veiga, F. Brezzi, and L. D. Marini. Virtual elements for linear elasticity problems. *SIAM Journal on Numerical Analysis*, 51(2):794–812, 2013.

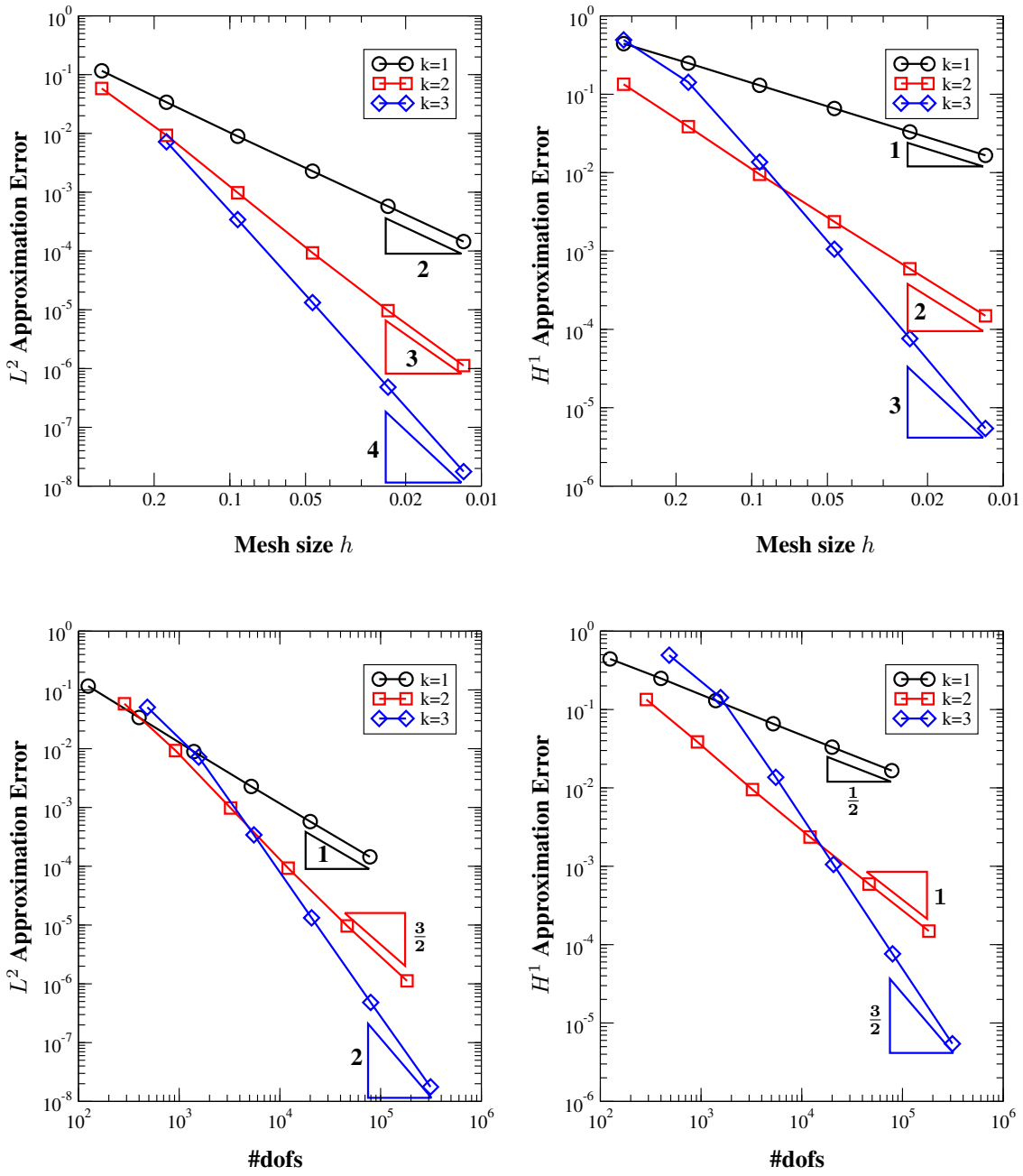

Fig. 2. Relative approximation errors obtained using the nonconforming VEM for $k = 1, 2, 3$ (from top to bottom). Calculations are carried out using the remapped hexagonal meshes of Figure 1(a). Errors are measured in the L^2 norm (left panels) and H^1 norm (right panels), and plotted versus h (top panels) and the number of degrees of freedom (right panels).

[9] L. Beirão da Veiga, F. Brezzi, L. D. Marini, and A. Russo. The hitchhiker's guide to the virtual element method. *Mathematical Models and Methods in Applied Sciences*, 24(8):1541–1573, 2014.

[10] L. Beirão da Veiga, F. Brezzi, L. D. Marini, and A. Russo. Virtual element methods for general second order elliptic problems on polygonal meshes. *Mathematical Models and Methods in Applied Sciences*, 26(04):729–750, 2015.

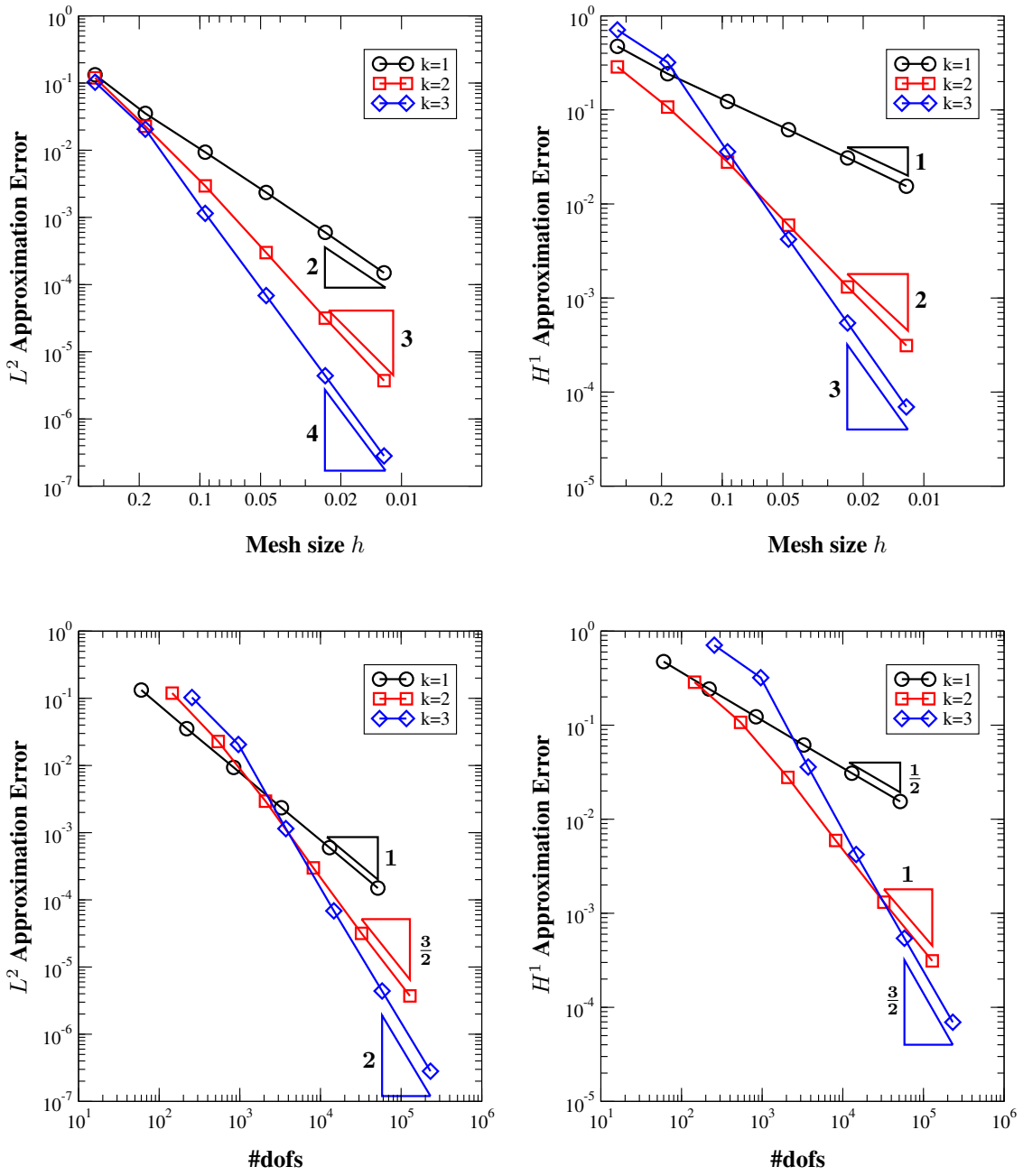

Fig. 3. Relative approximation errors obtained using the nonconforming VEM for $k = 1, 2, 3$ (from top to bottom). Calculations are carried out using the highly distorted quadrilateral meshes of Figure 1(b). Errors are measured in the L^2 norm (left panels) and H^1 norm (right panels), and plotted versus h (top panels) and the number of degrees of freedom (right panels).

[11] L. Beirão da Veiga, F. Brezzi, L. D. Marini, and A. Russo. H(div) and H(curl)-conforming VEM. *Numerische Mathematik*, 133(2):303–332, 2016.

[12] L. Beirão da Veiga, F. Brezzi, L. D. Marini, and A. Russo. Mixed virtual element methods for general second order elliptic problems on polygonal meshes. *ESAIM: Mathematical Modelling and Numerical Analysis*, 50(3):727–747, 2016.

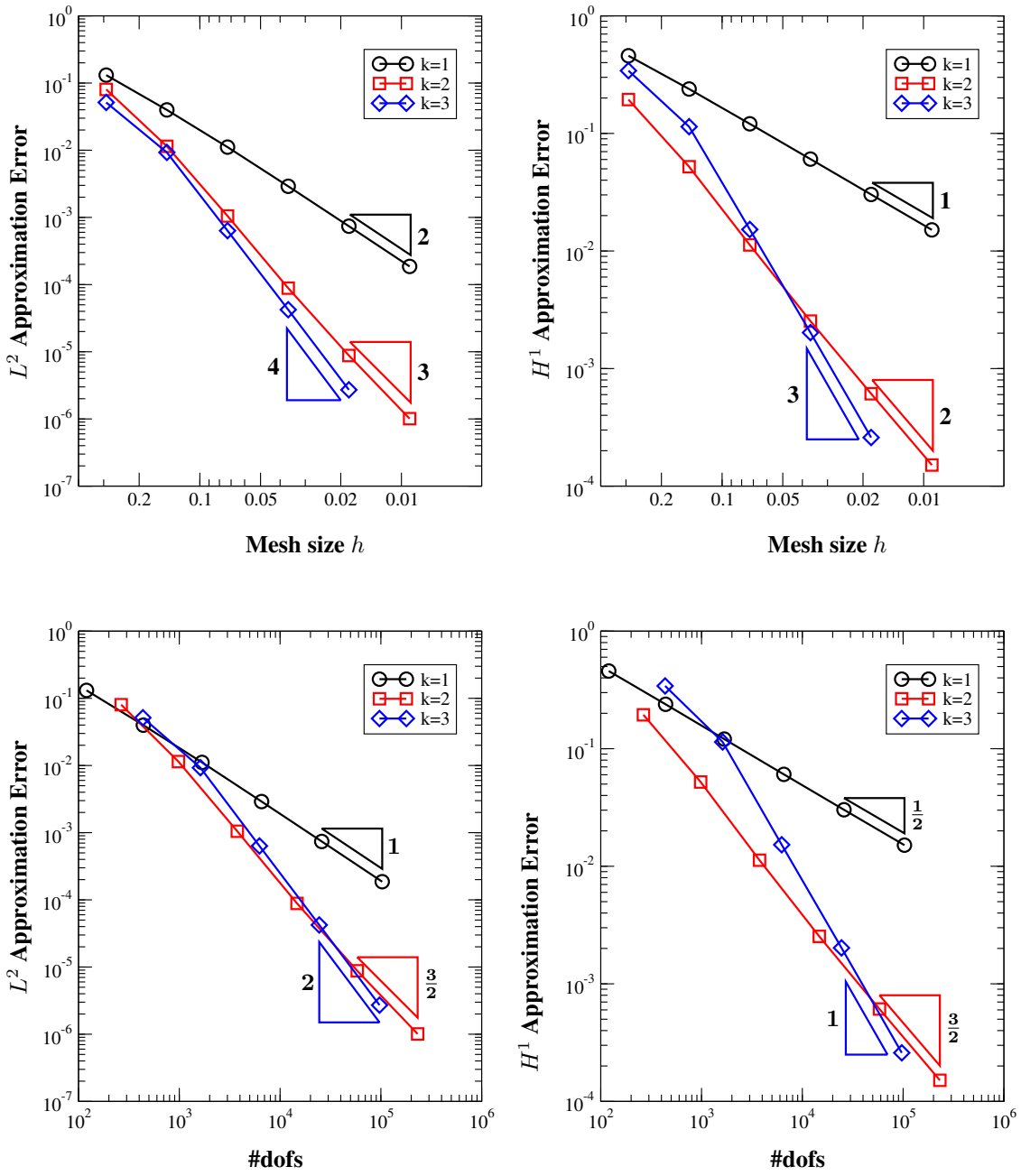

Fig. 4. Relative approximation errors obtained using the nonconforming VEM for $k = 1, 2, 3$ (from top to bottom). Calculations are carried out using the non convex meshes of Figure 1(c). Errors are measured in the L^2 norm (left panels) and H^1 norm (right panels), and plotted versus h. (top panels) and the number of degrees of freedom (right panels).

[13] L. Beirão da Veiga, F. Brezzi, L. D. Marini, and A. Russo. Serendipity nodal VEM spaces. *Computers and Fluids*, 141:2–12, 2016.

[14] L. Beirão da Veiga, F. Brezzi, L. D. Marini, and A. Russo. Virtual element methods for general second order elliptic problems on polygonal meshes. *Mathematical Models & Methods in Applied Sciences*, 26(4):729–750, 2016.

[15] L. Beirão da Veiga, A. Chernov, L. Mascotto, and A. Russo. Basic principles of hp virtual elements on quasiuniform meshes. *Mathematical Models & Methods in Applied Sciences*, 26(8):1567–1598, 2016.

[16] L. Beirão da Veiga, K. Lipnikov, and G. Manzini. Arbitrary order nodal mimetic discretizations of elliptic problems on polygonal meshes. *SIAM Journal on Numerical Analysis*, 49(5):1737–1760, 2011.

[17] L. Beirão da Veiga, K. Lipnikov, and G. Manzini. *The Mimetic Finite Difference Method*, volume 11 of *MS&A. Modeling, Simulations and Applications*. Springer, I edition, 2014.

[18] L. Beirão da Veiga, C. Lovadina, and G. Vacca. Divergence free virtual elements for the Stokes problem on polygonal meshes. *ESAIM: Mathematical Modelling and Numerical Analysis*, 51(2):509–535, 2017.

[19] L. Beirão da Veiga and G. Manzini. A virtual element method with arbitrary regularity. *IMA Journal on Numerical Analysis*, 34(2):782–799, 2014. DOI: 10.1093/imanum/drt018, (first published online 2013).

[20] L. Beirão da Veiga and G. Manzini. Residual a posteriori error estimation for the virtual element method for elliptic problems. *ESAIM: Mathematical Modelling and Numerical Analysis*, 49:577–599, 2015.

[21] L. Beirão da Veiga, G. Manzini, and M. Putti. Post-processing of solution and flux for the nodal mimetic finite difference method. *Numerical Methods for PDEs*, 31(1):336–363, 2015.

[22] M. F. Benedetto, S. Berrone, and A. Borio. The Virtual Element Method for underground flow simulations in fractured media. In *Advances in Discretization Methods*, volume 12 of *SEMA SIMAI Springer Series*, pages 167–186. Springer International Publishing, Switzerland, 2016.

[23] M. F. Benedetto, S. Berrone, A. Borio, S. Pieraccini, and S. Scialò. A hybrid mortar virtual element method for discrete fracture network simulations. *Journal of Computational Physics*, 306:148–166, 2016.

[24] M. F. Benedetto, S. Berrone, A. Borio, S. Pieraccini, and S. Scialo. The virtual element method for discrete fracture network flow and transport simulations. In *ECCOMAS Congress 2016 - Proceedings of the 7th European Congress on Computational Methods in Applied Sciences and Engineering*, volume 2, pages 2953–2970, 2016.

[25] M. F. Benedetto, S. Berrone, S. Pieraccini, and S. Scialò. The virtual element method for discrete fracture network simulations. *Computer Methods in Applied Mechanics and Engineering*, 280(0):135 – 156, 2014.

[26] S. Berrone, A. Borio, and G. Manzini. SUPG stabilization for the nonconforming virtual element method for advection-diffusion-reaction equations. *Computer Methods in Applied Mechanics and Engineering*, 340:500–529, 2018.

[27] S. Berrone, A. Borio, and S. Scialò. A posteriori error estimate for a PDE-constrained optimization formulation for the flow in DFNs. *SIAM Journal on Numerical Analysis*, 54(1):242–261, 2016.

[28] S. Berrone, S. Pieraccini, and S. Scialò. Towards effective flow simulations in realistic discrete fracture networks. *Journal of Computational Physics*, 310:181–201, 2016.

[29] S. Bertoluzza, M. Pennacchio, and D. Prada. Bddc and feti-dp for the virtual element method. *Calcolo*, 54:1565–1593, 2017.

[30] S. C. Brenner. Poincaré-Friedrichs inequalities for piecewise H^1 functions. *SIAM J. Numer. Anal.*, 41(1):306–324 (electronic), 2003.

[31] F. Brezzi, A. Buffa, and K. Lipnikov. Mimetic finite differences for elliptic problems. *ESAIM: Mathematical Modelling and Numerical Analysis*, 43(2):277295, 2009.

[32] A. Cangiani, E. H. Georgoulis, T. Pryer, and O. J. Sutton. A posteriori error estimates for the virtual element method. *Numerische Mathematik*, pages 1–37, 2017.

[33] A. Cangiani, V. Gyrya, and G. Manzini. The non-conforming virtual element method for the Stokes equations. *SIAM Journal on Numerical Analysis*, 54(6):3411–3435, 2016.

[34] A. Cangiani, V. Gyrya, G. Manzini, and O. Sutton. Chapter 14: Virtual element methods for elliptic problems on polygonal meshes. In K. Hormann and N. Sukumar, editors, *Generalized Barycentric Coordinates in Computer Graphics and Computational Mechanics*, pages 1–20. CRC Press, Taylor & Francis Group, 2017.

[35] A. Cangiani, G. Manzini, A. Russo, and N. Sukumar. Hourglass stabilization of the virtual element method. *International Journal on Numerical Methods in Engineering*, 102(3-4):404–436, 2015.

[36] A. Cangiani, G. Manzini, and O. Sutton. Conforming and nonconforming virtual element methods for elliptic problems. *IMA Journal on Numerical Analysis*, 37:1317–1354, 2017. (online August 2016).

[37] D. A. Di Pietro, J. Droniou, and G. Manzini. Discontinuous skeletal gradient discretisation methods on polytopal meshes. *Journal of Computational Physics*, 355:397–425, 2018.

[38] F. Gardini, G. Manzini, and G. Vacca. The nonconforming virtual element method for eigenvalue problems, 2018. arXiv:1802.02942v1.

[39] F. Gardini and G. Vacca. Virtual element method for second order elliptic eigenvalue problems. *IMA Journal on Numerical Analysis*, 2017. Preprint, arXiv:1610.03675.

[40] V. Gyrya, K. Lipnikov, and G. Manzini. The arbitrary order mixed mimetic finite difference method for the diffusion equation. *ESAIM: Mathematical Modelling and Numerical Analysis*, 50(3):851–877, 2016.

[41] Y. Kuznetsov, K. Lipnikov, and M. Shashkov. The mimetic finite difference method on polygonal meshes for diffusion-type problems. *Computational Geosciences*, 8(4):301–324, 2004.

[42] K. Lipnikov and G. Manzini. A high-order mimetic method on unstructured polyhedral meshes for the diffusion equation. *Journal of Computational Physics*, 272:360–385, 2014.

[43] K. Lipnikov, G. Manzini, J. D. Moulton, and M. Shashkov. The mimetic finite difference method for elliptic and parabolic problems with a staggered discretization of diffusion coefficient. *Journal of Computational Physics*, 305:111 – 126, 2016.

[44] K. Lipnikov, G. Manzini, and M. Shashkov. Mimetic finite difference method. *Journal of Computational Physics*, 257 – Part B:1163–1227, 2014. Review paper.

[45] G. Manzini, K. Lipnikov, J. D. Moulton, and M. Shashkov. Convergence analysis of the mimetic finite difference method for elliptic problems with staggered discretizations of diffusion coefficients. *SIAM Journal on Numerical Analysis*, 55(6):2956–2981, 2017.

[46] G. Manzini, A. Russo, and N. Sukumar. New perspectives on polygonal and polyhedral finite element methods. *Mathematical Models & Methods in Applied Sciences*, 24(8):1621–1663, 2014.

[47] S. Natarajan, P. A. Bordas, and E. T. Ooi. Virtual and smoothed finite elements: a connection and its application to polygonal/polyhedral finite element methods. *International Journal on Numerical Methods in Engineering*, 104(13):1173–1199, 2015.

[48] C. Paniconi, S. Ferraris, M. Putti, G. Pini, and G. Gambolati. Three-dimensional numerical codes for simulating groundwater contamination: FLOW3D, flow in saturated and unsaturated porous media. In P. Zannetti, editor, *Computer Techniques in Environmental Studies V, Vol. 1: Pollution Modeling*, pages 149–156, Southampton, UK, 1994. Computational Mechanics Publications.

[49] E. Süli and D. F. Mayers. *An introduction to numerical analysis*. Cambridge University Press, Cambridge, UK, 2003.

[50] V. Thomée. *Galerkin Finite Element Methods for Parabolic Problems*, volume Lecture Notes in Mathematics, 1054 of *Springer Series in Computational Mathematics 25*. Springer Berlin Heidelberg, 2nd ed edition, 1997.

[51] O. Čertík, F. Gardini, G. Manzini, and G. Vacca. The virtual element method for eigenvalue problems with potential terms on polytopic meshes. *Applications of Mathematics*, 63(3):333365, 2018.

[52] G. Vacca and L. Beirão da Veiga. Virtual element methods for parabolic problems on polygonal meshes. *Numerical Methods for Partial Differential Equations. An International Journal*, 31(6):2110–2134, 2015.

[53] P. Wriggers, W. T. Rust, and B. D. Reddy. A virtual element method for contact. *Computational Mechanics*, 58(6):1039–1050, 2016.

[54] J. Zhao, S. Chen, and B. Zhang. The nonconforming virtual element method for plate bending problems. *Mathematical Models & Methods in Applied Sciences*, 26(9):1671–1687, 2016.